Research Square

Preprints are preliminary reports that have not undergone peer review.
They should not be considered conclusive, used to inform clinical practice,
or referenced by the media as validated information.

Exploration of the evolving role of ^{18}F-FDG PET/CT in evaluating extrahepatic cholangiocarcinoma lymph node metastasis

Zhihui Gao
Zhongshan hospital fudan university
Jie Xiao
Zhongshan hospital fudan university
Cheng Jin
Zhongshan hospital fudan university
Yiqiu Zhang
Zhongshan hospital fudan university
Tao Suo
Zhongshan hospital fudan university
Xiaojian Ni
Zhongshan hospital fudan university
Houbao Liu
zsliuhb@sina.com
Zhongshan Hospital Fudan University https://orcid.org/0000-0002-8159-9988
Sheng Shen
Zhongshan hospital fudan university
Hongcheng Shi
Zhongshan hospital fudan university

Research Article

Keywords: extrahepatic cholangiocarcinoma, 18F-FDG PET/CT, lymph nodes metastasis, predictive model

Posted Date: April 19th, 2026

DOI: https://doi.org/10.21203/rs.3.rs-9326457/v1

License: This work is licensed under a Creative Commons Attribution 4.0 International License.
Read Full License

Abstract

Purpose: The presence of lymph node metastases at diagnosis is one of the most relevant negative prognostic factors in patients with extrahepatic cholangiocarcinoma (eCCA). This study aims to identify the diagnostic criteria of ^{18}F-FDG PET/CT for lymph node metastasis in eCCA, and to develop a more accurate predictive model of lymph node metastasis based on these results.

Methods: All pathologically diagnosed cases of 98 lymph nodes from 71 patients of extrahepatic cholangiocarcinoma preoperatively were retrospectively analyzed. The distributional differences between malignant and benign groups were compared. The variables for constructing the metastasis prediction model of the lymph nodes were determined through further univariate and multivariate analyses of the variables exhibiting distributional differences.

Results: It was observed that lymph nodes with tumor metastasis displayed greater size and metabolism. Following multifactorial analysis, a lymph node metastasis prediction model comprising of three variables: short diameter, aspect ratio and SUVmax. This model demonstrated favorable outcomes in our cohort's validation (AUC 0.932, sensitivity 87.5%, specificity 90.3%). In addition, these factors were used to construct the nomogram model, which showed good concordance and accuracy.

Conclusion: In this study, a lymph node metastasis prediction model for extrahepatic cholangiocarcinoma based on short diameter, aspect ratio, and SUVmax has been developed. However, a larger sample size and a multicenter study are necessary to authenticate the model's efficacy.

Introduction

Extrahepatic cholangiocarcinoma (eCCA) comprises a group of cancers that originate from the extrahepatic biliary tree and can be categorized as hilar and distal cholangiocarcinoma based on anatomic location. According to the American Cancer Society's predictions for 2023, the United States is expected to witness 12,220 new cases and 5,410 deaths related to eCCA[1–2]. Globally, the incidence rate of eCCA has been gradually increasing, with Asia reporting the highest rate at 0.55–2.24 per 100,000 person-years[3–4]. Concurrently, the mortality rate remains high and median overall survival (OS) in all eCCA patients was 8 months during 1973 through 2012[5] .

Currently, radical adequate surgical resection (R0) is the only potentially curative treatment for patients with eCCA, though a large portion eventually die from tumor recurrence and lymph node metastasis. The 2023 national comprehensive cancer network (NCCN) guidelines pointed out that lymph node metastases are independent predictors of the prognosis after resection, and lymph node dissection in the hilar region and pancreatic head is also part of the radical resection[6]. In eCCA, approximately 40–53% of patients experience lymph node metastasis, making it a critical risk factor for determining the surgical approach and assessing tumor recurrence[7]. Furthermore, the number of metastatic lymph nodes is related to prognosis. For the 8th edition of the American Joint Committee on Cancer (AJCC),

the N category has been more accurate and harmonized for gallbladder, perihilar bile ducts, distal bile duct, ampulla, and pancreas. N1 is defined as one to three metastatic lymph nodes, and N2 as four or more metastatic lymph nodes[8]. Consequently, precise assessment of lymph node status in eCCA using reliable imaging tools holds paramount importance in guiding treatment decisions and predicting patients' prognoses. X-ray computed tomography (CT) scan and magnetic resonance imaging (MRI) play a pivotal role in primary screening, diagnosis and staging. These modalities are used to reflect the anatomic and morphological changes of primary tumor and related lymph nodes. Node size (short-axis diameter) is the major evaluation criterion, but the size of benign and malignant lymph nodes overlaps. Morphological features provide additional information, which do not exist in early stage and in micro-metastasis. MRI-based apparent diffusion coefficient (ADC) measurements, particularly the tumor ADC value and the tumor-to-lymph node ADC ratio, show potentially promising. However, there was no difference in terms of ADC value between benign lymph nodes and those with metastatic in case of cholangiocarcinoma[9]. Altogether, CT and MRI may be inconclusive in a considerable fraction of patients except for late stage.

Positron emission tomography (PET) is a pharmacokinetic-based functional imaging modality that provides valuable insights into the metabolism of different body regions through the distribution of the tracer ^{18}F-fluorodeoxyglucose (^{18}F-FDG). Tumor cells are known to have enhanced glycolytic activity and increased uptake of glucose and ^{18}F-FDG. This non-invasive method can provide metabolic and anatomical information almost simultaneously. Notably, ^{18}F-FDG PET/CT has been extensively utilized in the diagnosis of lymph node staging in various solid cancers, due to its advantages in anatomical and functional imaging and non-invasive nature[10–11]. In cases of non-small cell lung cancers, the application of ^{18}F-FDG PET/CT yielded estimated sensitivity and specificity rates of 81.3% and 79.4%, respectively[10]. Furthermore, the ^{18}F-FDG PET/CT nomogram incorporating metabolic parameters and radiomics score showed moderate improvement of the efficiency for lymph node staging[13]. Studies have suggested that ^{18}F-FDG/PET can be helpful in diagnosing regional lymph node metastasis and distant metastasis of eCCA, while also showing potential value in evaluating tumor relapse. However, it's important to note that ^{18}F-FDG PET/CT may produce false-positive results in patients with bile duct infections rather than eCCA. Due to its limited specificity, ^{18}F-FDG-PET has a constrained role in assessing the primary tumor, and there are currently no standardized positive criteria to evaluate regional lymph node metastasis in eCCA[14–15] .

To the best of our knowledge, there is very little analysis that investigated radiomics features and metabolic parameters based on lymph nodes for prediction in eCCA. In this study, we conducted an investigation using ^{18}F-FDG PET/CT examinations in eCCA patients and aimed to identify diagnostic criteria for differentiating between benign and malignant lymph nodes.

Methods

Patients

This single-center retrospective study was approved by the ethics committee of Fudan University (approval number: B2023-299R2). This study included patients who were diagnosed with eCCA, underwent ^{18}F-FDG PET/CT scan preoperatively and received radical surgery at Zhongshan Hospital, Fudan University from January to December 2019. Patients with a history of other types of tumors, prior treatment for eCCA, no confirmed histopathological biopsy of lymph nodes, ^{18}F-FDG PET/CT conducted in other hospitals, a time interval of more than one month between ^{18}F-FDG PET/CT scan and surgery, or those with no identified lymph nodes in the ^{18}F-FDG PET/CT were excluded. In the end, a total of 98 lymph node data from 71 eCCA patients were included in this study.

^{18}F-FDG PET/CT imaging technique

All patients were required to be fasted for at least 6 h before PET/CT imaging and blood glucose concentration was less than 11.0 mmol/L, and then they were intravenously administered ^{18}F-FDG (3.7 to 5.6 MBq/kg). ^{18}F-FDG was purchased from CSBio (Shanghai, China) Ltd. All acquisitions were performed on Discovery VCT 64 system (GE Healthcare, Milwaukee, Wis, USA), uMI550, or uMI780 PET/CT system (United Imaging Healthcare, Shanghai, China) approximately 50–60 min after intravenous administration. The whole-body CT scanning parameters were set as follows: tuber current (120 mA), voltage (140 kV), and scan layer thickness (3.75 mm). The PET scan was performed after CT scan acquisition and conducted in 6 or 7 bed positions. Immediately after CT image acquisition, PET data were acquired for 2 min per table position in 3D mode. Image datasets for PET were reconstructed iteratively by applying the CT data for attenuation correction, and coregistered images displayed on a workstation.

Clinical, biopsy and imaging data

The clinical and biopsy data of the patients, encompassing age, gender, preoperative diagnosis, and intraoperative histopathological biopsy, were collected retrospectively from the electronic medical record system of Zhongshan Hospital. According to the conformed biopsy results, the lymph nodes were retrospectively marked in the preoperative imaging data. The lymph nodes were confirmed by surgeons involved in the surgery and nuclear medicine doctors together. The imaging parameters of both the primary tumor and the marked lymph nodes were recorded, including the size of the primary tumor, CT, as well as the long and short diameters of the lymph nodes. The SUVmax of ^{18}F-FDG PET/CT was automatically calculated by computer software. The tumor-to-liver background ratio (TLBR) and tumor-to-blood pool ratio (TBR) were calculated using the following expression: TLBR= SUVmax/SUVbackground(liver), TBR= SUVmax/SUVbackground(blood). The lesion was segmented by the adaptive threshold (50%), and then metabolic tumor volume (MTV), total lesion glycolysis (TLG) value were automatically calculated and generated. Discrepancies between surgeons and nuclear medicine doctors were resolved by consensus.

Statistical analysis

Statistical analyses were conducted by the authors using SPSS version 25.0 (IBM Corp., Armonk, NY, USA). Categorical data and Continuous variables were presented and analyzed as described previously[16]. To identify the best cutoff for distinguishing patients with lymph node metastasis, a receiver-operating characteristic (ROC) were generated, and the area under the ROC curve (AUC), sensitivity, specificity were used to investigate the validity diagnostic models. Binary logistic analysis and multivariate logistic regression analysis were employed to identify variables that could predict tumor lymph node metastasis. Differences with a *p* value <0.05 were considered statistically significant. According to the final logistic regression model and by using the rms package in R version 3.4.2 (http://www.r-project.org/), the nomogram model was constructed as described previously[12, 17].

Results

Characteristics of patients

The process of patients inclusion was visualized in **Fig. 1**. Ultimately, this study was enrolled 71 eCCA patients (median age, 63 years, 51 males and 18 females) and comprehensively found 98 lymph node data from these patients. These patients were divided into present or absent group and the lymph nodes were divided into lymph node (+) or (-) group according to the pathological results. There was no significant difference in the clinical characteristics between these patients, as shown in **Table 1**. Among the 71 patients, there were 35 perihilar cholangiocarcinoma (pCCA), 28 distal cholangiocarcinoma (dCCA), 4 gallbladder cancer (GBC), and 2 of ampullary carcinomas. While not achieving statistical significance, it is of interest to note that patients exhibiting lymph node metastasis tended to have larger primary tumor volumes (3.15 ± 2.57 cm *vs* 2.21 ± 1.13, $p = 0.263$), and a younger age (59.7 ± 10.0 *vs* 63.9 ± 8.5, $p = 0.079$).

Differences in the distribution of imaging data among eCCA patients

In the pursuit of identifying variables that can serve as indicators of the lymph node metastasis status in patients with eCCA, radiological data were compared (**Table 2**). Initially, an analysis was conducted to assess the distribution of these data between the lymph node (+) group and lymph node (−) group. The measurements of the long and short diameters were utilized to quantify the size of lymph nodes ascertained from CT. Remarkably, lymph node (+) group displayed elongated short diameters of lymph nodes (11.3 ± 2.8 mm *vs* 7.5 ± 1.8, $p < 0.001$) and smaller aspect ratio (1.2 ± 0.1 *vs* 1.6 ± 0.5, $p < 0.001$, **Fig. 2**). There was statistically different in the SUVmax of lymph node between present and absent lymph nodes (3.8 ± 2.2 vs 2.3 ± 1.0, p < 0.001, **Table 2**). There was no significant difference in the SUVmax of the primary tumor between both cohorts, and the SUVmax of the abdominal aorta was significant（2.0 ± 0.6 vs 2.2 ± 0.5, $p < 0.001$）.The other ^{18}F-FDG PET/CT features including MTV, TLG and TBR, were significant different between groups (**Table 2** and **Fig. 2** all $p < 0.001$).

Construction of the eCCA lymph node metastasis prediction model

Further analysis was conducted both on the clinical information and imaging data. Univariate analysis and ROC curves were performed for each factor to predict the status of lymph node. Short diameter, lymph node aspect ratio, SUVmax, TBR, MTV, and TLG were associated with lymph node metastasis (**Table 3** and **Fig. 3**). Notably, the short diameters, TLG, lymph node aspect ratio and TBR exhibited the highest AUC of the ROC curves (0.872, 0.852, 0.844, and 0.810, respectively, all $p < 0.001$). Multivariable analysis was conducted on variables with $p < 0.05$ in the univariate analysis. Ultimately, three variables were identified to construct the predictive model: short diameters (odd ratio [OR] 1.71, 95% confidence interval [CI]1.17-2.49), aspect ratio (OR 0.05, 95% CI 0.00-1.00) and SUVmax (OR 2.19, 95% CI 1.14-4.19) (**Table 3**). Utilize this model to validate the cohorts included in this study, the AUC of the ROC curve was 0.932 (95% CI 0.878-0.986, **Fig. 4A**, **Table 4**). The sensitivity and specificity were 87.5% and 90.3%, respectively. The nomogram for this predictive model can be found in **Fig. 4C**.

The prediction effect of the prediction model in pCCA and dCCA

Within the patient cohort examined in this study, it was observed that the rate of lymph node metastasis stood higher among patients with pCCA (28.57%), in comparison to those with dCCA (17.86%). However, it's noteworthy that this disparity did not attain statistical significance (**Table 1**). To gain deeper insights into potential variations in the factors influencing lymph node metastasis between these two subtypes, the validation of the lymph node metastasis predictive model was pursued individually for patients with pCCA and dCCA. Impressively, the predictive model exhibited an AUC of 0.991 for pCCA patients **(Fig.4B)**, surpassing the AUC of 0.783 for dCCA (**Table 4**). This notable contrast underscores the presence of distinct factors contributing to lymph node metastasis between patients with pCCA and those with dCCA.

For a more comprehensive exploration of the optimal predictive models for pCCA and dCCA patients, additional rounds of univariate and multivariable regression analyses on each subgroup were performed (**Table 5** & **Sulp.table 1**), and subsequently constructed predictive models for both categories. Following the necessary adjustments, the lymph node aspect ratio and TLG were chosen to build the predictive model for pCCA patients. This model was validated within its respective cohort, demonstrating an AUC of 0.991 (**Table 6**). This discovery showcased a superior lymph node metastasis predictive model for pCCA patients.

However, when considering patients with dCCA, the pursuit of a dependable predictive model persisted as a challenge, even after the implementation of adjustments. It is postulated that this challenge could be ascribed to the constrained size of the sample, which introduces plausible errors into the analysis. Future efforts should focus on amassing a larger sample size and incorporating additional clinical and imaging data to develop a more robust predictive model for lymph node metastasis in dCCA patients.

Discussion

This research assessing diagnostic criteria of ^{18}F-FDG PET/CT for lymph node metastasis for eCCA in a retrospective single-center study. The investigation offers invaluable insights pertaining to the prognostication of lymph node metastasis, thereby furnishing crucial information to inform clinical decision-making processes.

eCCA is characterized by its potential for lymph node metastasis. The extent of lymph node involvement not only determines patient prognosis but also influences treatment strategies. While ^{18}F-FDG PET/CT has been employed as a metabolic imaging modality to reflect lymph node status in non-small cell lung cancer and other solid cancers, there still exists a lack of well-defined diagnostic criteria to assess lymph node metastasis status in patients with eCCA. It is easy to diagnose cases where lymph node with FDG accumulation significantly increased, but the point is to expand the utility of FDG-PET/CT when FDG accumulation is slight. In this study, we successfully developed a lymph node metastasis prediction model for eCCA utilizing patients' ^{18}F-FDG PET/CT alongside other imaging data. Additionally, we undertook calibration of the prediction model specifically for the pCCA subtype. However, further investigation into the prediction model for the dCCA subtype necessitates a larger sample size.

This investigation unveiled discernible disparities in the distribution of radiological parameters among cohorts of patients preoperative diagnosed with eCCA, segregating them based on the presence or absence of lymph node metastasis. Of particular note, lymph nodes harboring tumor metastases manifested a tendency towards increased short diameters (present 11.3 ± 2.8 mm, absence 7.5 ± 1.8 mm, $p < 0.001$). Noteworthy, the SUVaorta exhibited elevated values within the lymph node metastasis group, implying a potential impact of lymph node metastasis on the glucose metabolism proficiency of the aortic territory. Furthermore, lymph nodes afflicted with tumor metastasis also demonstrated heightened glucose uptake capabilities as evidenced by greater SUVmax (present 3.8 ± 2.2, absence 2.3 ± 1.0, $p < 0.001$), accompanied by an overall escalation in metabolic vigor. This was particularly evident in the metastasis group, which exhibited augmented levels of MTV, TLG and TBR.

The final lymph node metastasis prediction model developed for eCCA encompasses three variables: lymph node short diameters, lymph node SUVmax and the aspect ratio of lymph node. Notably, the short diameters and SUVmax level exhibit a positive correlation with the occurrence of lymph node metastasis, while the lymph node aspect ratio demonstrates a negative correlation. These three variables effectively capture distinct aspects of lymph node characteristics: the short diameters reflect overall size, the aspect ratio signifies overall shape, and SUVmax represents glucose uptake capacity (metabolic activity) of the lymph node. Based on this predictive model, it is postulated that larger lymph nodes with a more circular shape and higher SUVmax in eCCA patients are more likely to harbor tumor metastasis.

For patients with pCCA, the variables ultimately included in the prediction model were adjusted to aspect ratio and TLG. While these exhibited high efficacy in internal validation (AUC 0.991, 95% CI 0.969-1.000), they did not demonstrate significance in multivariate regression and failed to adequately reflect the relevant relationship with lymph node metastasis. Additionally, a predictive model suitable for patients

with dCCA could not be successfully constructed. Therefore, the primary limitations of this study encompass: 1. Its single-center design with a limited sample size; 2. The absence of appropriate internal and external validation cohorts, thereby restricting the extrapolation capability of the lymph node metastasis prediction model.

In conclusion, ^{18}F-FDG PET/CT holds potential in predicting tumor lymph node metastasis. Through the utilization of imaging and ^{18}F-FDG PET/CT data from eCCA patients, we established a prediction model for tumor lymph node metastasis. This model evaluates lymph node status from the perspectives of size, shape, and glucose metabolism, aiding in a more accurate assessment of the preoperative condition for patients with eCCA.

Abbreviations

AUC: area under curve; CI: confidence interval; dCCA: distal cholangiocarcinoma; eCCA: extrahepatic cholangiocarcinoma; ^{18}F-FDG PET/CT: ^{18}F-fluorodeoxyglucose with positron emission tomography/computed tomography; GBC: gallbladder cancer; MTV: metabolic tumor volume; NCCN: national comprehensive cancer network; OR: odd ratio; pCCA: perihilar cholangiocarcinoma; ROC: receiver operating characteristic; SUVmax: maximum standardized uptake value; TBR: tumor background ratio; TBR2: SUVmax/SUVaorta; TBR3: SUVmax/SUVprimary; TLG: total lesion glycolysis.

Declarations

Conflict of interest:

All authors declare that no conflict of interest is associated with this work.

References

1. Siegel RL, Miller KD, Wagle NS, Jemal A. Cancer statistics, 2023. **CA Cancer J Clin 2023**, 73(1): 17-48.
2. Elvevi A, Laffusa A, Scaravaglio M, Rossi RE, Longarini R, Stagno AM, et al. Clinical treatment of cholangiocarcinoma: an updated comprehensive review. **Ann Hepatol 2022**, 27(5): 100737.
3. Florio AA, Ferlay J, Znaor A, Ruggieri D, Alvarez CS, Laversanne M, et al. Global trends in intrahepatic and extrahepatic cholangiocarcinoma incidence from 1993 to 2012. **Cancer 2020**, 126(11): 2666-2678.
4. Banales JM, Marin J, Lamarca A, Rodrigues PM, Khan SA, Roberts LR, et al. Cholangiocarcinoma 2020: the next horizon in mechanisms and management. **Nat Rev Gastroenterol Hepatol 2020**, 17(9): 557-588.

5. Mukkamalla S, Naseri HM, Kim BM, Katz SC, Armenio VA. Trends in Incidence and Factors Affecting Survival of Patients With Cholangiocarcinoma in the United States. **J Natl Compr Canc Netw 2018**, 16(4): 370-376.
6. Benson AB, D'Angelica MI, Abrams T, Abbott DE, Ahmed A, Anaya DA, et al. NCCN Guidelines(R) Insights: Biliary Tract Cancers, Version 2.2023. **J Natl Compr Canc Netw 2023**, 21(7): 694-704.
7. Nitta N, Ohgi K, Sugiura T, Okamura Y, Ito T, Yamamoto Y, et al. Prognostic Impact of Paraaortic Lymph Node Metastasis in Extrahepatic Cholangiocarcinoma. **World J Surg 2021**, 45(2): 581-589.
8. Chun YS, Pawlik TM, Vauthey JN. 8th Edition of the AJCC Cancer Staging Manual: Pancreas and Hepatobiliary Cancers. **Ann Surg Oncol 2018**, 25(4): 845-847.
9. Turkes F, Dere O, Dinc F, Yazkan C, Ozcan O, Nazli O. The Efficacy of MRI-Based ADC Measurements in Detecting Axillary Lymph Node Metastasis: Evaluation of a Prospective Study. **Curr Oncol 2024**, 31(11): 6598-6607.
10. Schmidt-Hansen M, Baldwin DR, Hasler E, Zamora J, Abraira V, Roque IFM. PET-CT for assessing mediastinal lymph node involvement in patients with suspected resectable non-small cell lung cancer. **Cochrane Database Syst Rev 2014**, 2014(11): CD009519.
11. Moore JL, Subesinghe M, Santaolalla A, Green M, Deere H, Van Hemelrijck M, et al. Metabolic tumour and nodal response to neoadjuvant chemotherapy on FDG PET-CT as a predictor of pathological response and survival in patients with oesophageal adenocarcinoma. **Eur Radiol 2023**, 33(5): 3647-3659.
12. Xie Y, Zhao H, Guo Y, Meng F, Liu X, Zhang Y, et al. A PET/CT nomogram incorporating SUVmax and CT radiomics for preoperative nodal staging in non-small cell lung cancer. **Eur Radiol 2021**, 31(8): 6030-6038.
13. Wartski M, Sauvanet A. 18F-FDG PET/CT in pancreatic adenocarcinoma: A role at initial imaging staging? **Diagn Interv Imaging 2019**, 100(12): 735-741.
14. Lamarca A, Barriuso J, Chander A, Mcnamara MG, Hubner RA, Oreilly D, et al. (18)F-fluorodeoxyglucose positron emission tomography ((18)FDG-PET) for patients with biliary tract cancer: Systematic review and meta-analysis. **J Hepatol 2019**, 71(1): 115-129.
15. Pang L, Mao W, Zhang Y, Liu G, Hu P, Chen S, et al. Comparison of (18)F-FDG PET/MR and PET/CT for pretreatment TNM staging of hilar cholangiocarcinoma. **Abdom Radiol (NY) 2023**, 48(8): 2537-2546.
16. Gao Z, Wang J, Shen S, Bo X, Suo T, Ni X, et al. The impact of preoperative biliary drainage on postoperative outcomes in patients with malignant obstructive jaundice: a retrospective analysis of 290 consecutive cases at a single medical center. **World J Surg Oncol 2022**, 20(1): 7.
17. Lv J, Liu YY, Jia YT, He JL, Dai GY, Guo P, et al. A nomogram model for predicting prognosis of obstructive colorectal cancer. **World J Surg Oncol 2021**, 19(1): 337.

Tables

Tables 1 to 6 are available in the Supplementary Files section.

Figures

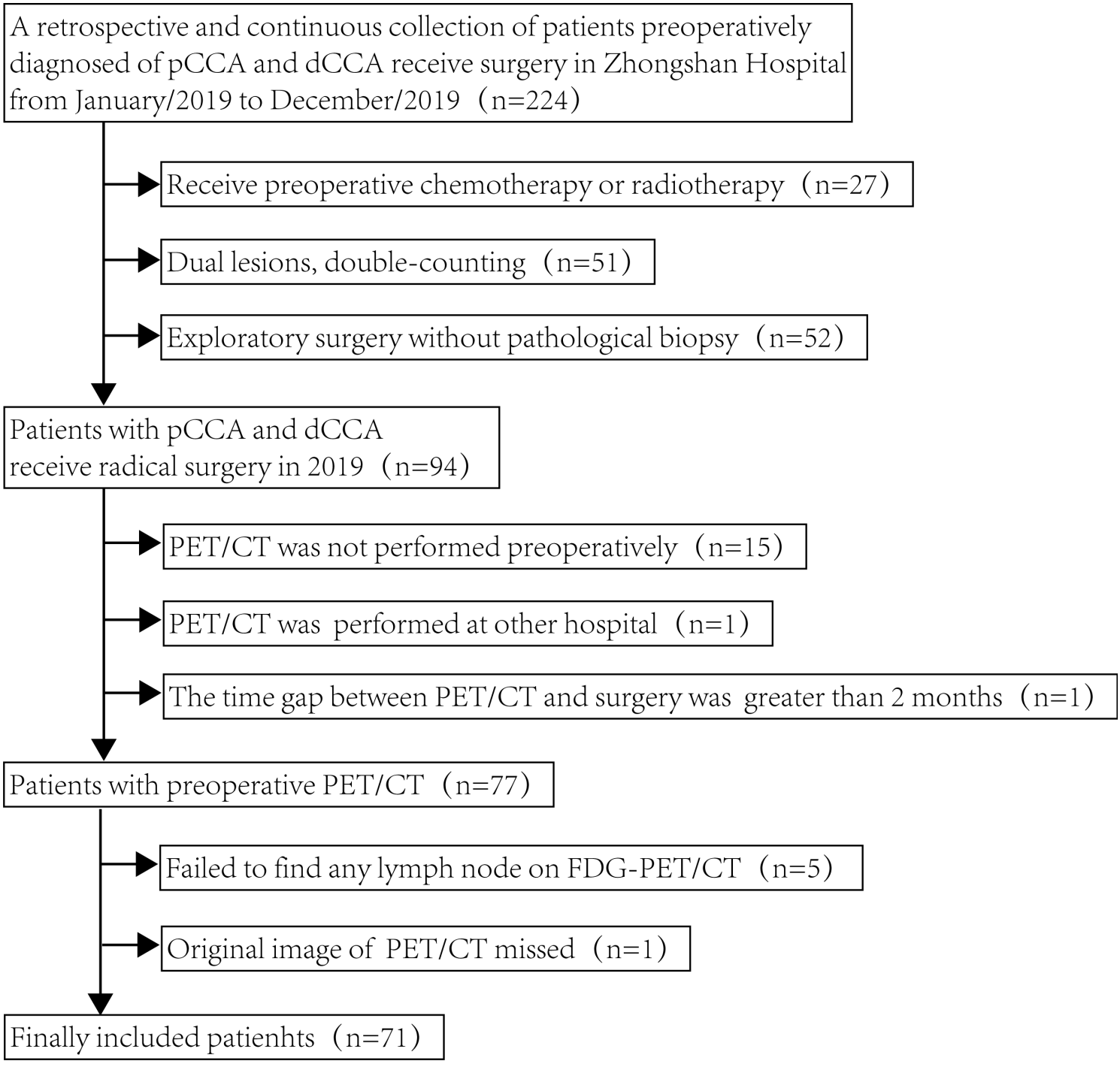


Figure 1

Flowchart of the enrolled patients.

Abbreviations in this illustration: dCCA: distal cholangiocarcinoma; ^{18}F-FDG PET/CT: ^{18}F-fluorodeoxyglucose with positron emission tomography/computed tomography; pCCA: perihilar

cholangiocarcinoma.

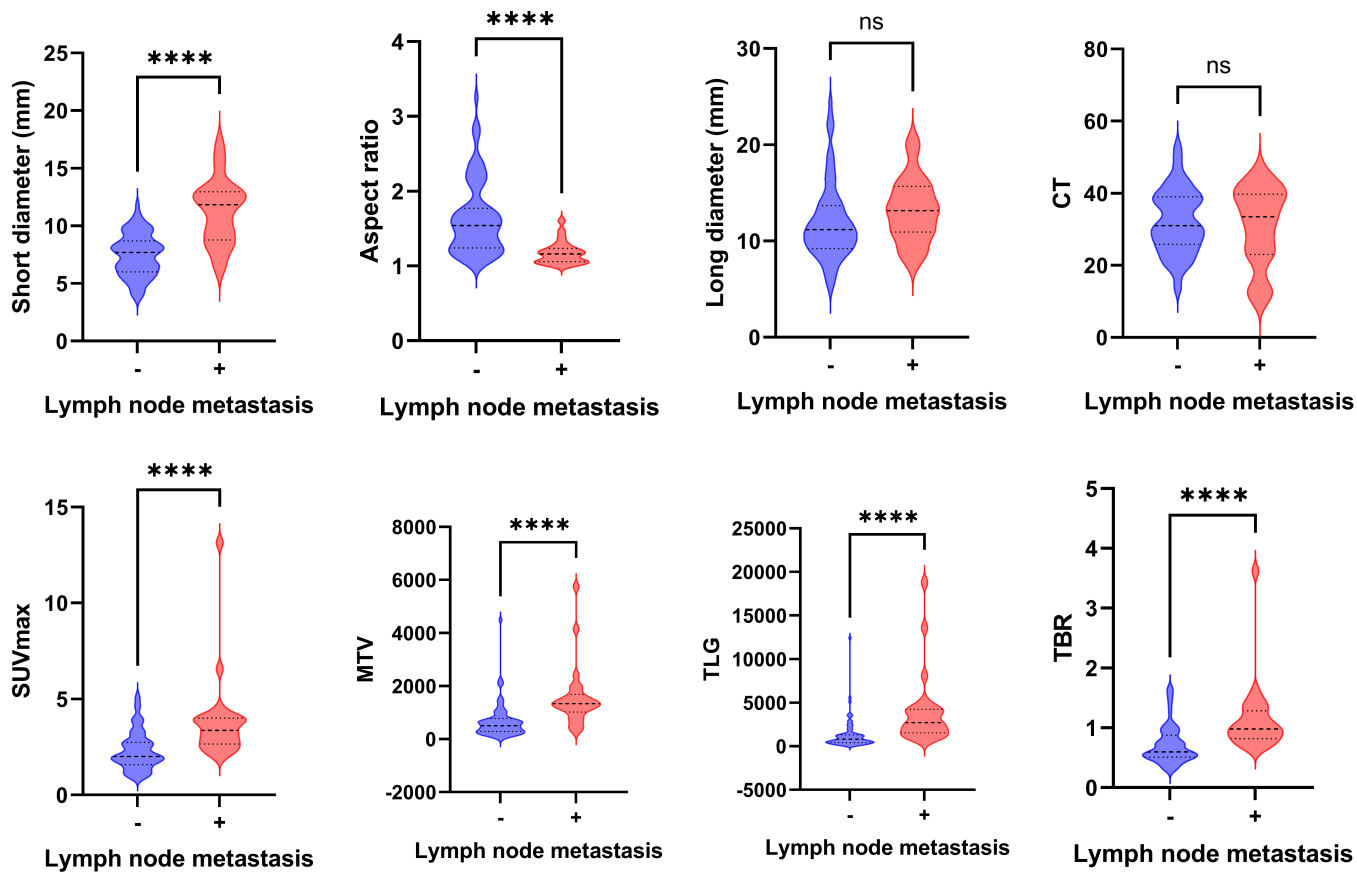


Figure 2

Differences in the distribution of imaging data among eCCA patients. Lymphatic metastasis from eCCA with greater short diameters ($P < 0.001$) and smaller aspect ratio ($P < 0.001$); B ^{18}F-FDG/PET data of lymph nodes in patients with eCCA.

Abbreviations in this illustration: MTV: metabolic tumor volume; SUVmax: maximum SUV; TBR: target-to-blood pool ratio; TLG: total lesion glycolysis.

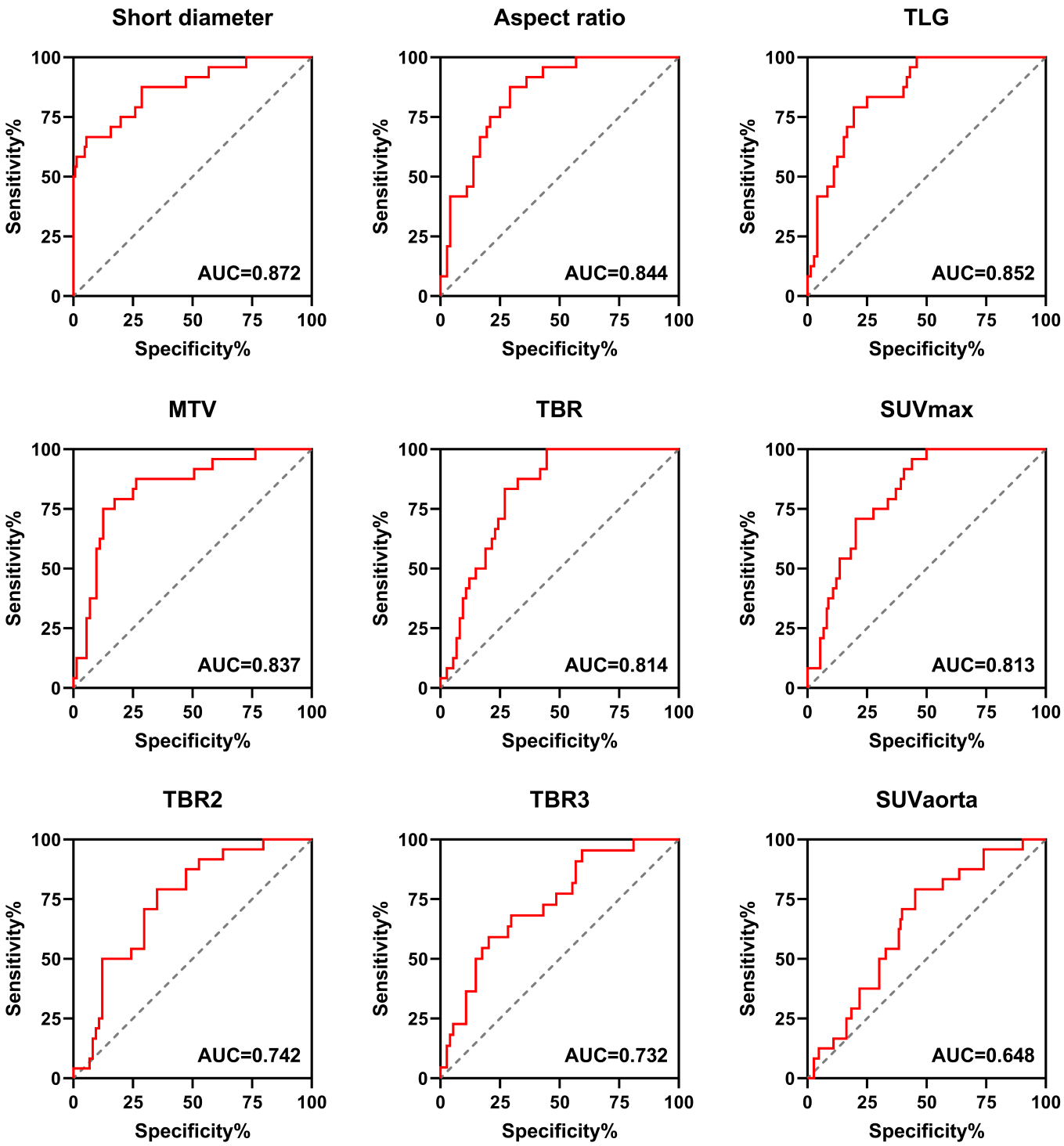


Figure 3

ROC curves for statistically significant variables after univariate analysis.

Abbreviations in this illustration: MTV: metabolic tumor volume; SUVaorta: abdominal aorta SUV; SUVmax: maximum SUV; TBR: target–to–blood pool ratio; TBR2: SUVmax/SUVaorta; TBR3: SUVmax/SUVprimary; TLG: total lesion glycolysis.

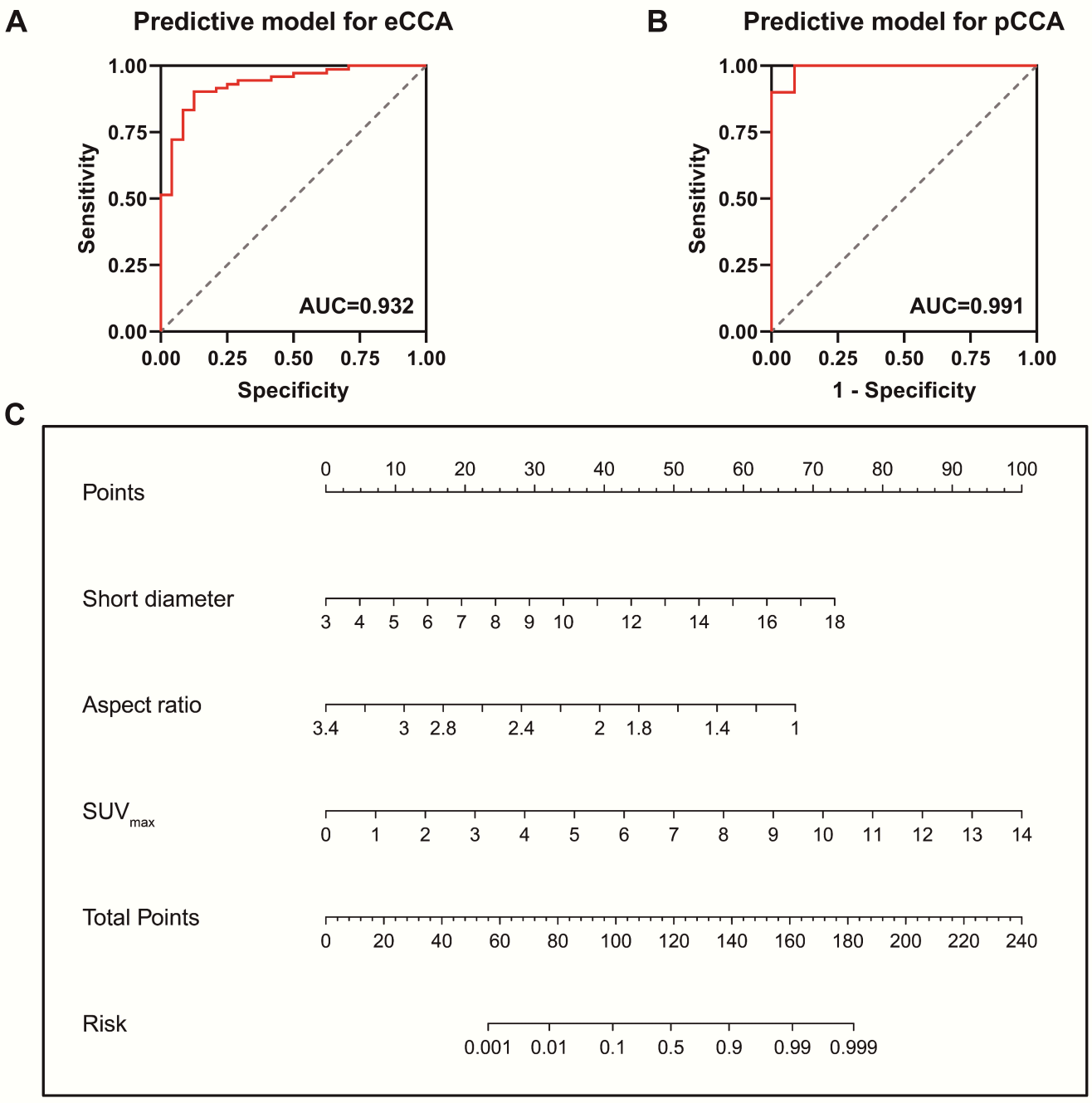


Figure 4

ROC curves for lymph node metastasis prediction models and the nomogram.

A Predictive model for eCCA (AUC 0.932); B Calibrated predictive model for pCCA (AUC 0.991); C Nomogram of the predictive model for eCCA.

Abbreviations in this illustration: AUC: area under curve; SUVmax: maximum SUV.

Supplementary Files

This is a list of supplementary files associated with this preprint. Click to download.

- Table1.docx
- Table2.docx
- Table3.docx
- Table4.docx
- Table5.docx
- Table6.docx
- Sulp.docx